

The mc-Si wafers (1.5 Ωcm boron doped) used for lifetime samples originate from the same mc-Si ingot and the same ingot height as the investigated standard industrial 156x156 mm² mc-Si PERC solar cell, leading to a comparable material quality of the initial material. Sister wafers (5x5 cm²) with comparable grain and defect structure were used to compare the influence of different process steps on degradation and regeneration behaviour of the lifetime samples. A scheme of the applied process sequences is given in Fig. 1. The wafers were chemically etched to remove saw damage. Sample A was not further processed and only a surface passivation was realized by firing of a plasma-enhanced chemical vapour deposition (PECVD) SiN_x:H layer. For samples B, C, and D different gettering sequences were applied. Sample B was gettered by a POCl₃ diffusion (55 Ω/\square), while sample C was gettered by screen-printing and firing of an Al contact on the backside. P- and Al-gettering was combined in case of sample D. Additionally, a PECVD SiN_x:H layer was applied to all bare wafer surfaces to protect the wafers from contamination during the following firing step. Afterwards, the SiN_x:H layers as well as the Al back surface field and the emitter were removed. The samples were surface passivated again by firing (measured wafer temperature: 730°C) of a PECVD SiN_x:H layer (same deposition parameters as before) leading to an additional hydrogenation of the investigated samples.

For degradation, lifetime samples as well as the solar cell are held at a temperature of approx. 75°C on a hot plate under illumination with halogen lamps (0.9±0.05 suns for lifetime samples, 1±0.05 sun for the solar cell). During the degradation and regeneration process the solar cell is characterized in situ by automated open circuit voltage (V_{oc}) measurements. For lifetime samples, effective minority charge carrier lifetime (τ_{eff}) is measured repetitively by the fast and self-calibrated time resolved photoluminescence imaging (TR-PLI) method [10, 11] at room temperature, resulting in a series of spatially resolved lifetime maps for each sample over degradation time. The first τ_{eff} data point of the lifetime samples is measured directly (approx. 2 min) after the last firing step consistent with standard solar cell characterization, which takes usually place directly after firing in industrial production lines.

For a statistically relevant analysis of areas differing in material quality, the TR-PLI lifetime maps of each sample over time are aligned and an array of 2,500 areas (each 150x150 μm^2 in size) at fixed positions is distributed over the TR-PLI lifetime map of the 5x5 cm² mc-Si samples to get good statistics. Average τ_{eff} values within these areas are extracted over degradation time and further analyzed. This method allows tracking of changes in τ_{eff} of different sample areas under degradation conditions. The advantage of this approach is that the spatially resolved information of τ_{eff} maps over degradation time can be easily displayed. The τ_{eff} data for each 150x150 μm^2 area on the samples is plotted over time and coded by a rainbow colour bar based on the areas' lifetime values at the beginning of the degradation experiment.

3 RESULTS AND DISCUSSION

Continuously measured V_{oc} data of an industrial mc-Si PERC solar cell are shown in Fig. 2. It is obvious that this PERC solar cell is LeTID sensitive and the V_{oc} data shows a degradation of approx. 12% rel. after 200 h followed by regeneration as also observed previously, e.g., in [3]. After 1500 h the solar cell recovers almost completely. As already discussed in, e.g., [1, 3] the observed degradation and regeneration cannot be fully explained by BO-correlated degradation or FeB pair dissociation processes.

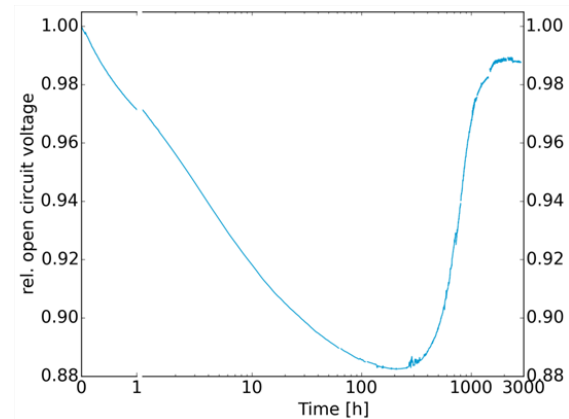


Figure 2: Continuously measured V_{oc} data of an industrial mc-Si PERC solar cell showing degradation and regeneration (first 1 h: linear scale, afterwards: log scale).

Fig. 3 shows the behaviour of harmonically averaged τ_{eff} for the four different processed lifetime sister samples A-D. All samples show fast degradation within the first minutes which could be attributed to FeB- and/or BO-based degradation effects. After longer periods, significant differences are measured for samples A, B, C, and D regarding the strength of the degradation, the range of minimum and maximum τ_{eff} in dependence of the degradation state, and the regeneration behaviour which can be clearly observed for sample A and also slightly for samples C and D. The ungettered sample A shows the strongest degradation but also the strongest relative regeneration. Applied gettering steps (samples B, C, D) reduce the degradation effect significantly. While samples with Al-gettering step (sample C and D) show a lifetime minimum due to degradation, no clear minimum could be observed in case of the only P-gettered sample B.

First investigations on a set of gallium doped mc-Si lifetime samples with and without P-gettering step result in a slower degradation at the beginning of the experiment, most probably due to missing BO- or FeB-induced degradation, strengthening the hypothesis that other impurities are responsible for the so called LeTID effect, as already observed by Ramspeck *et al.* [1] on solar cell level. Also for gallium doped lifetime samples, the degradation in ungettered samples is more pronounced compared to P-gettered samples [12].

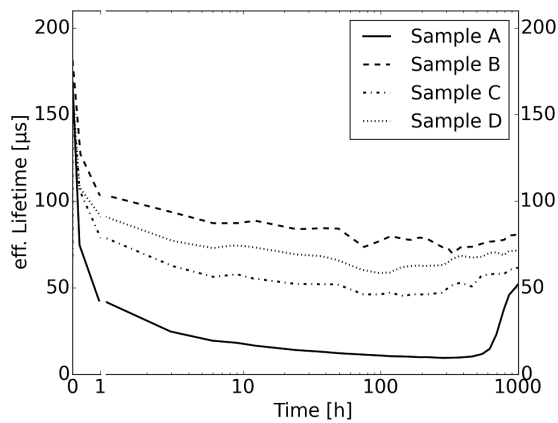


Figure 3: Harmonically averaged τ_{eff} data for differently processed mc-Si wafers. Degradation and regeneration behaviour of lifetime samples can be strongly influenced by previously applied gettering sequences (first 1 h: linear scale, afterwards: log scale).

A comparison to the degradation behaviour of the solar cell shows that the maximum degradation level for average τ_{eff} in Fig. 3 and the V_{oc} value in case of the solar cell (Fig. 2) is reached after approximately the same degradation time using (almost) the same illumination level and elevated temperature. This leads to the assumption that the underlying degradation and regeneration effect can be studied either on lifetime or on solar cell level.

The disadvantage of average τ_{eff} analyses is that information on local lifetime distribution measured by spatially resolved TR-PLI gets lost. Fig. 4 shows exemplarily τ_{eff} maps of sample A at three different states: at the beginning of the degradation, in the degraded state, and during the regeneration process. The whole series of these spatially resolved TR-PLI measurements have been aligned and analyzed as described above.

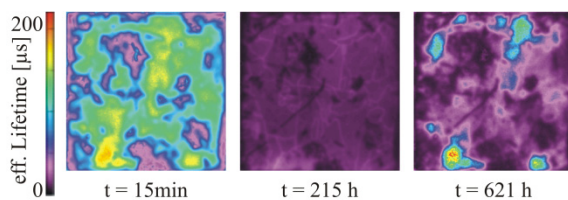


Figure 4: Spatially resolved TR-PLI measurements of sample A at the beginning of the applied degradation process, in the degraded state and during regeneration.

Further analyses of the degradation and regeneration behaviour will be discussed based on Fig. 5. Each single line (guides to the eye connecting single data points) in Fig. 5 represents one of the 2,500 small $150 \times 150 \mu\text{m}^2$ areas on the lifetime samples.

The applied colour code, based on the initial lifetime of each sample at the beginning of the experiment, shows that for all four samples the relative τ_{eff} distribution is maintained during the experiment, which means that independently of the applied process sequence, sample areas with the highest initial τ_{eff} show also the highest τ_{eff} at the maximum degradation level as well as during the regeneration process. This holds true even if the range of

lifetime is narrowed down during degradation or is spread again during regeneration.

In case of sample A (not gettered, Fig. 5a), a very strong and fast degradation of the whole sample is observed. As already mentioned for harmonic average τ_{eff} data, FeB- and/or BO-induced degradation could be involved additionally to LeTID in the first few minutes, but the degradation behaviour cannot be fully explained based on FeB- and/or BO-induced dynamics. Especially sample areas of higher initial τ_{eff} suffer from the applied degradation conditions, and relative degradation in these areas is stronger than in sample areas with lower initial τ_{eff} .

The initial lifetime distribution of sample A (approx. 30–350 μs) narrows down to a very small range (approx. 5–30 μs) at maximum degradation level. This strong degradation even in areas of initially high τ_{eff} could be explained by an approximately homogenous formation of defects over the wafer area. The degradation kinetics is very similar in all sample areas, independently of the initial τ_{eff} . After approximately 300 h a regeneration process sets in, with regeneration in areas with higher initial τ_{eff} (red lines) starting significantly earlier than in areas of lower initial τ_{eff} , indicated by a black dashed line in Fig. 5a, and also by the inlay and the differently coloured arrows in Fig. 5a. The earlier onset of regeneration in areas of initially high τ_{eff} is the reason why in these regions the minimal visible τ_{eff} level is reached earlier compared to areas with lower initial τ_{eff} . But it has to be assumed that initially good τ_{eff} areas show very similar degradation kinetics (time constants) than initially poor τ_{eff} areas. The different starting points for observable regeneration are remarkable, especially regarding the narrow τ_{eff} distribution at around 200 h. The different regeneration behaviour leads to the assumption that the regeneration is not only a reversal of the first degradation reaction and that the underlying mechanism is more complex. It is not yet clear whether τ_{eff} recovers completely.

Up to now it is not yet clear whether the observed degradation within the first hours under illumination originates from bulk defect formation or changes in surface passivation quality. Therefore, an additional sample is prepared exactly like sample A, and the same degradation conditions are applied leading to a comparable degradation behaviour as observed for sample A. After approx. 300 h, the $\text{SiN}_x\text{:H}$ surface passivation layer is etched back and a chemical surface passivation (iodine ethanol, [13]) is applied. The previously measured spatial distribution of low τ_{eff} values after 300 h degradation is thereby confirmed, verifying that the observed strong degradation is a bulk effect and not related to changes in $\text{SiN}_x\text{:H}$ surface passivation quality. There are hints that $\text{SiN}_x\text{:H}$ surface passivation quality slightly decreases after several hundred hours under illumination at 75°C. This might influence the long time regeneration behaviour (>1000 h), but cannot explain the observed degradation.

The P-gettered sample B (Fig. 5b) shows only a slight lifetime reduction within the first minutes under illumination at elevated temperature and is therefore significantly less sensitive to LeTID than sample A. In contrast to the ungettered sample A discussed above, the τ_{eff} range (approx. 40–360 μs) is only slightly narrowed down and stays nearly constant during the experiment.

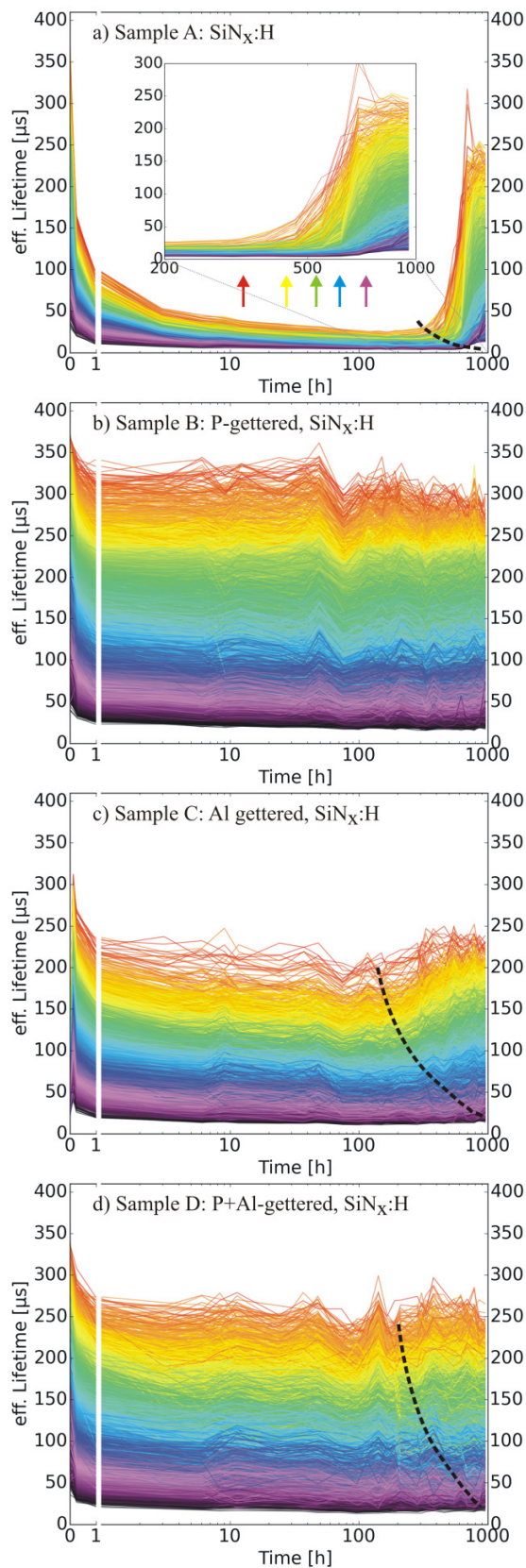


Figure 4: τ_{eff} of differently processed sister wafers (first 1 h: linear scale, afterwards: log scale). Each line in the graph represents an area of $150 \times 150 \mu\text{m}^2$ in the spatially resolved TR-PLI lifetime measurements and is colour-coded to its value at the beginning of degradation. Black dashed lines indicate beginning regeneration.

The data shows no clear maximum degradation level and no regeneration, and τ_{eff} stays almost constant in the different sample areas. Areas of lower initial lifetime after gettering show more relative degradation than areas of higher material quality.

In case of sample B, the repetition of the PECVD $\text{SiN}_x\text{:H}$ deposition and firing as shown in Fig. 1 has been performed to get a similar temperature load compared to the Al-gettered samples C and D. If the degradation conditions are applied to a P-gettered sample after the first firing of the $\text{SiN}_x\text{:H}$ passivation layer, comparable results to sample B are observed on an additional wafer set with comparable initial material quality. If the investigated sample area is strongly dominated by extended defect clusters of lower material quality, a more pronounced degradation could be observed also for P-gettered samples (not shown). This hints towards a complex interaction of gettering efficiency on local defect structures (as seen, *e.g.*, in [14]) and the effect on degradation behaviour.

In contrast to sample B, the Al-gettered sister sample C shows a significantly different degradation and regeneration behaviour. Overall degradation and regeneration behaviour is closer to the ungettered sample A than to the P-gettered sample B. As observed for sample A, the Al-gettered sample C shows also a maximum degradation level and a narrowing of the τ_{eff} range, but by far not as significant as sample A. The regeneration process again sets in earlier for sample areas with higher initial τ_{eff} as indicated by a black dashed line in Fig. 5c.

For sample D, both Al- and P-gettering were applied. Degradation is stronger than in case of sample B but less pronounced compared to sample C. Also a beginning regeneration can be hinted as indicated by a black dashed line in Fig. 5d. Therefore, the degradation and regeneration behaviour of sample D is a mix of the observed results of the only P-gettered sample B and the only Al-gettered sample C.

Due to the expected different contamination level or impurity distribution of the gettered samples B, C, and D compared to sample A, it is assumed that impurities strongly influence the degradation and regeneration behaviour. A P-gettering step seems to be more efficient to remove degradation sensitive defects than an Al-gettering step. After P-gettering, each following temperature step leads to a redistribution of (internally or externally) gettered degradation relevant defects. Besides firing steps, the temperature loads during surface passivation processing steps have to be taken into account. In [15], P-gettered lifetime samples with different surface passivation treatments (including stack systems like $\text{AlO}_x + \text{SiN}_x\text{:H}$ and a thermal SiO_2 covered by $\text{SiN}_x\text{:H}$) are compared. It can be demonstrated that for samples with additional temperature load after the P-gettering step a more pronounced LeTID and following regeneration occurs. The effect is most pronounced for a thermal SiO_2 step with the highest temperature load, followed by samples with additional AlO_x deposition, while samples with single PECVD $\text{SiN}_x\text{:H}$ layer show a similar behaviour as discussed above for sample B.

It has to be mentioned that the firing conditions (set parameters) are kept constant but lead to a slightly different temperature load of the bulk material during the first firing step for sample B compared to samples C and D due to the screen-printed Al back side of samples C and D. The lower wafer temperature of the P-gettered

sample B compared to the additional Al gettered sample D during the first firing step may lead to a slightly different and less LeTID sensitive impurity distribution for sample B. As shown in [9], different firing temperatures generally have an influence on degradation behaviour.

The earlier onset of regeneration for LeTID in areas of higher τ_{eff} resembles the behaviour of regeneration of BO-correlated degradation. There it could be shown that a higher excess charge carrier density Δn in the Si bulk leads to a faster regeneration process [6, 7]. Interestingly, the onset of LeTID regeneration starts earlier in the best quality areas of sample C (after approx. 200 h), having higher τ_{eff} as compared to the best areas of sample A (after approx. 400 h) as indicated by the dashed line in Fig. 5, with sample D lying in between. Note that all samples are sister wafers with comparable extended defect structure and similar surface passivation quality. As higher τ_{eff} leads to higher Δn for constant illumination, this leads to the conclusion that Δn might play a decisive role for LeTID regeneration.

The next step in the analogy between regeneration for LeTID and BO regeneration would be the assumption that hydrogen plays an important role, too. As shown for BO regeneration, the presence of hydrogen in the Si bulk seems to be a prerequisite for the regeneration to occur and its concentration influences the regeneration kinetics [16]. The significantly different time scale could, e.g., be explained by the different effective diffusion constant of hydrogen at relatively low temperatures in mc-Si compared to monocrystalline Si due to trapping (trap assisted diffusion). But this hypothesis still has to be confirmed in future experiments.

4 MODEL FOR LeTID AND CONSEQUENCES

Effective gettering seems to be a key component to minimize the impact of LeTID in mc-Si. Under the assumption that degradation in mc-Si at longer timescales (>1 h at 75°C) is triggered by the concentration of a specific impurity (or a mix of impurities) that is more or less homogeneously distributed over the wafer area, a first rough model can be introduced.

In areas of good material quality (low density of extended defects like grain boundaries and/or dislocations) where gettering is very effective, LeTID can be suppressed very effectively in lifetime samples. In contrast, in areas of poorer crystal quality (more extended defects), gettering is less effective as impurities might also be present in form of precipitates that are harder to getter externally, because they first have to be dissolved, and dissolved impurities might be gettered internally again at extended defects. This can be seen qualitatively for sample B (Fig. 5b), where good sample areas show less relative degradation than areas of poorer quality, and is also observed in [17] for a different set of samples and different processing sequences.

A consequence of this first model is that high temperature steps after the gettering steps might lead to a redistribution of gettered impurities from their initial gettering sites (e.g., the emitter region, internal gettering sites). Indeed, it could be observed that a thermal oxidation step carried out after a P-gettering step “reactivates” LeTID and following regeneration [15].

The model presented here is most probably not yet able to explain LeTID and regeneration behaviour in all

its facets, but gettering seems to play an important role and should be considered in further experiments to deepen the understanding of LeTID in mc-Si.

The regeneration observed for LeTID might be related to the presence of hydrogen in the Si bulk, being more mobile under illumination, maybe due to the change of its charge state [18, 19].

Another consequence from the proposed model is that a back-to-back P-diffusion process as normally carried out in industrial cell processing might lead to a stronger LeTID effect due to the less effective gettering.

5 SUMMARY AND OUTLOOK

The influence of different solar cell gettering steps on LeTID and regeneration has been demonstrated using spatially resolved data from TR-PLI. It could be shown that the behaviour of lifetime samples resembles the behaviour of PERC solar cells fabricated from the same mc-Si material and can therefore be regarded as relevant for PERC-type solar cell processing.

The applied data processing allows the analysis of different sample areas over degradation time in a statistically relevant way and is not limited to selected sample areas or the comparison of only two degradation or regeneration states.

For ungettered samples, it could be shown that degradation kinetics are very similar for all sample areas irrespective of their initial quality, while regeneration sets in first in good quality areas. Gettering drastically reduces LeTID while the strength of degradation and the following regeneration is influenced by the applied gettering sequence. P-gettering is more efficient than Al-gettering for removing or restructuring LeTID sensitive defects, but gettering efficacy depends also on the underlying crystal defect structure.

It could be shown that LeTID is a bulk degradation effect occurring in boron as well as gallium doped mc-Si. Therefore, it cannot be attributed to BO- or FeB-related defects alone.

The influence of the different gettering sequences on the degradation and regeneration process leads to the conclusion that the concentration and distribution of (metal) impurities play a major role for LeTID and regeneration. Therefore, the industrial PERC solar cell processing sequence should be optimized concerning effective gettering and avoidance of redistribution of gettered impurities during following temperature steps. In addition, a high concentration of hydrogen in the correct binding state might help to speed up the regeneration process (as for BO regeneration [20]), when LeTID cannot be avoided completely.

This long time experiment is still running to further analyze the regeneration process and the long time stability of the regenerated state and the surface passivation. Also, additional lifetime samples with further process sequences are under investigation.

6 ACKNOWLEDGEMENT

The authors would like to thank Lisa Mahlstaedt and David Sperber for help during sample processing and Axel Herguth for help during sample characterization and fruitful discussions. Part of this work was funded by the German Federal Ministry of Economic Affairs and

Energy and by industrial partners within the research project "SolarLIFE" (0325763B) and within 0325581. The content is the responsibility of the authors.

7 REFERENCES

- [1] K. Ramspeck, S. Zimmermann, H. Nagel, A. Metz, Y. Gassenbauer, B. Birkmann, A. Seidl, Light induced degradation of rear passivated mc-Si solar cells. Proc. 27th EU PVSEC, 2012, 861-865.
- [2] F. Fertig, K. Krauss, S. Rein, Light-induced degradation of PECVD aluminium oxide passivated silicon solar cells, Phys. Stat. Sol. RRL 9(1) (2014) 41-46.
- [3] F. Kersten, P. Engelhart, H.C. Ploigt, A. Stekolnikov, T. Lindner, F. Stenzel, M. Bartzsch, A. Szpeth, K. Petter, J. Heitmann, J. Müller, Degradation of multicrystalline silicon solar cells and modules after illumination at elevated temperature, Sol. En. Mat. & Sol. Cells 2015 142 (2015) 83-86.
- [4] M.A. Green, K. Emery, Y. Hishikawa, W. Warta, E.D. Dunlop, Solar cell efficiency tables (version 47), Progr. Photovolt.: Res. Appl. 24(1) (2016) 3-11.
- [5] A. Herguth, G. Schubert, M. Kaes, G. Hahn, A new approach to prevent the negative impact of the metastable defect in boron doped Cz silicon solar cells, Proc. 4th WCPEC, 2006, 940-943.
- [6] A. Herguth, G. Schubert, M. Kaes, G. Hahn, Investigations on the long time behavior of the metastable boron-oxygen complex in crystalline silicon, Progr. Photovolt.: Res. Appl. 16 (2008) 135-140.
- [7] A. Herguth, G. Hahn, Kinetics of the boron-oxygen related defect in theory and experiment, J. Appl. Phys. 108 (2010) 114509.
- [8] K. Krauss, F. Fertig, D. Menzel, S. Rein, Light-induced degradation of silicon solar cells with aluminium oxide passivated rear side, En. Procedia 77 (2015) 599-606.
- [9] D. Bredemeier, D. Walter, S. Herlufsen, J. Schmidt, Lifetime degradation and regeneration in multicrystalline silicon under illumination at elevated temperature, AIP 6 (2016) 035119.
- [10] D. Kiliani, G. Micard, B. Steuer, B. Raabe, A. Herguth, G. Hahn, Minority charge carrier lifetime mapping of crystalline silicon wafers by time-resolved photoluminescence imaging, J. Appl. Phys. 110 (2011) 054508.
- [11] D. Kiliani, A. Herguth, G. Micard, J. Ebser, G. Hahn, Time-resolved photoluminescence imaging with electronic shuttering using an image intensifier unit, Sol. En. Mat. & Sol. Cells 106 (2012) 55-59.
- [12] A. Zuschlag, D. Skorka, G. Hahn, Comparison of degradation and regeneration kinetics in differently doped mc-Si materials, to be published.
- [13] K. Pollock, J. Junge, G. Hahn, Detailed investigation of surface passivation methods for lifetime measurements on silicon wafers, IEEE J. Photovolt. 2(1) (2012) 1-6.
- [14] S. Gindner, P. Karzel, B. Herzog, G. Hahn, Efficacy of phosphorus gettering and hydrogenation in multicrystalline silicon, IEEE J. Photovolt. 4(4) (2014) 1063-1070.
- [15] A. Zuschlag, D. Skorka, G. Hahn, Degradation and regeneration analysis in mc-Si, Proc. 43rd IEEE PVSC, 2016, in press.
- [16] S. Wilking, A. Herguth, G. Hahn, Influence of hydrogen on the regeneration of boron-oxygen related defects in crystalline silicon, J. Appl. Phys. 113 (2013) 194503.
- [17] D. Skorka, A. Zuschlag, G. Hahn, Spatially resolved degradation and regeneration kinetics in mc-Si, this conference.
- [18] P. Hamer, B. Hallam, S. Wenham, M. Abbott, Manipulation of hydrogen charge states for passivation of p-type wafers in photovoltaics, IEEE J. Photovolt. 4(5) (2014) 1252-1260.
- [19] C. Sun, F.E. Rougieux, D. Macdonald, A unified approach to modelling the charge state of monatomic hydrogen and other defects in crystalline silicon, J. Appl. Phys. 117 (2015) 045702.
- [20] S. Wilking, A. Herguth, G. Hahn, Influence of bound hydrogen states on BO-regeneration kinetics and consequences for high-speed regeneration processes, Sol. En. Mat. & Sol. Cells 131 (2014) 2-8.